Critical Refractions

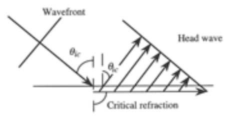

Figure 2-16 A wave that strikes an interface at its critical angle θ_{ic} is refracted parallel to the interface producing what is commonly referred to as a head wave.

ing upward at velocity V_1. This wave generally is referred to as the *head wave*, and any of its rays also are at the critical angle (Fig. 2-16).

mined by

$$\theta_{ic} = \sin^{-1}\left(\frac{V_1}{V_2}\right) \qquad (2\text{-}27)$$

As before, it is trivial to prove that this general form also holds for all cases of refraction such as refracted shear waves produced by incident compressional waves.

Refraction, Reflection versus Angle of Incidence

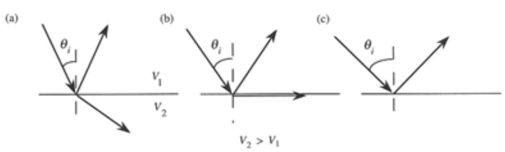

Figure 2-17 (a) Incident, reflected, and refracted rays. (b) Increasing θ_i results in a critically refracted ray. (c) Increasing θ_i still further produces total reflection.

Diffractions

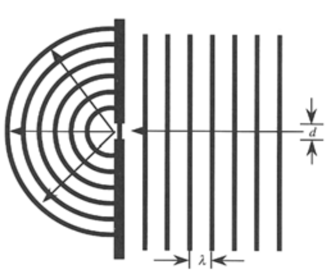

Diffractions

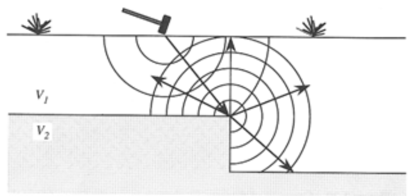

Ray Paths

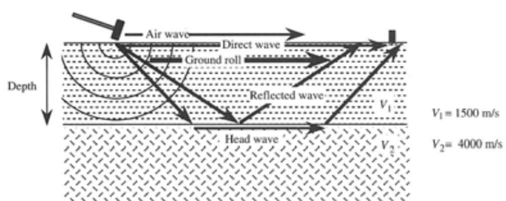

Figure 2-20 Generalized diagram illustrating ray paths for waves included in Table 2-4. Included are the direct wave, reflection, critical refraction, the air wave, and ground roll. All waves are compressional with the exception of ground roll.

Distance versus Time

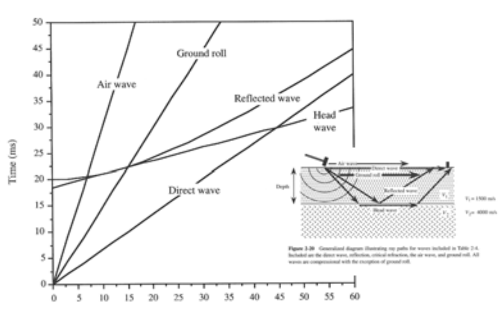

Distance versus Time (Wavelets)

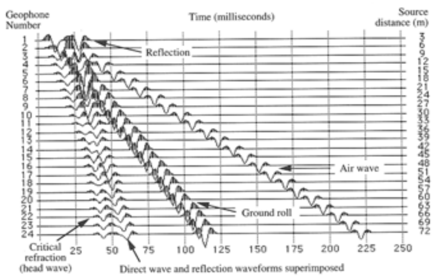

Energy Loss: Spherical Spreading

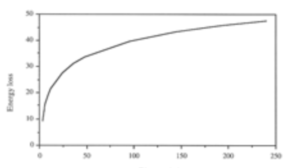

Figure 2-23 Energy losses in decibels due to spherical spreading at various distances from an energy source.

TABLE 2-5 Energy Losses Due to Spherical Spreading

Distance from shot (m)	**3**	**6**	**9**	**12**	**12**	**24**	**36**	**48**	**48**	**96**	**144**	**192**	**240**
Spherical spreading loss (db)	9.54	15.56	19.08	21.58	21.58	27.60	31.13	33.62	33.62	39.65	43.17	45.67	47.60
Loss from previous point (db)		6.02	3.52	2.50		6.02	3.52	2.50		6.02	3.52	2.50	1.94

Energy Loss: Absorption

TABLE 2-6 Energy Losses (in decibels) Due to Absorption

Frequency (Hz)	Compressional Wave				Shear Wave			
	Distance (m)							
	10	60	120	240	10	60	120	240
5	0.0293	0.1755	0.351	0.702	0.0585	0.351	0.702	1.404
10	0.0585	0.351	0.702	1.404	0.117	0.702	1.404	2.808
30	0.1755	1.053	2.106	4.212	0.351	2.106	4.212	8.424
100	0.585	3.51	7.02	14.04	1.17	7.02	14.04	28.08
200	1.17	7.02	14.04	28.08	2.34	14.04	28.08	56.16
300	1.755	10.53	21.06	42.12	3.51	21.06	42.12	84.24

P-wave velocity (m/s)	**4000**
S-wave velocity (m/s)	**2000**
Absorption coefficient	0.55 db/wavelength

$$I = I_0 e^{-qr} \qquad (2\text{-}28)$$

Energy Loss: Splitting

However, if P-wave incidence is normal to the interface, the equations reduce to a very simple form. No S-waves are generated under normal incidence. The ratios of the amplitudes A are

$$\frac{A_{rfl}}{A_i} = \frac{\rho_2 V_2 - \rho_1 V_1}{\rho_2 V_2 + \rho_1 V_1} \qquad \frac{A_{rfr}}{A_i} = \frac{2\rho_1 V_1}{\rho_2 V_2 + \rho_1 V_1} \qquad (2\text{-}29)$$

where the quantities are as diagramed in Figure 2-24. These equations often are shortened to the form

$$\frac{A_{rfl}}{A_i} = \frac{Z_2 - Z_1}{Z_2 + Z_1} \qquad \frac{A_{rfr}}{A_i} = \frac{2Z_1}{Z_2 + Z_1} \qquad (2\text{-}30)$$

where $Z_1 = \rho_1 V_1$ and $Z_2 = \rho_2 V_2$

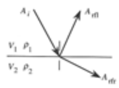

Figure 2-24 Illustration of quantities used in simple form of Zoeppritz' equations.

Reflection Coefficients

TABLE 2-7 Reflection Coefficients for P-wave at Normal Incidence

Density (g/cm3)—layer 1	**2.00**
Density (g/cm3)—layer 2	**2.60**
P-wave velocity (m/s)—layer 1	**1500**
P-wave velocity (m/s)—layer 2	**4500**

Z1	3000
Z2	11700

Reflection coefficient	0.59	Energy fraction reflected	0.35
Refraction coefficient	0.41	Energy fraction refracted	0.65

Reflection Coefficients

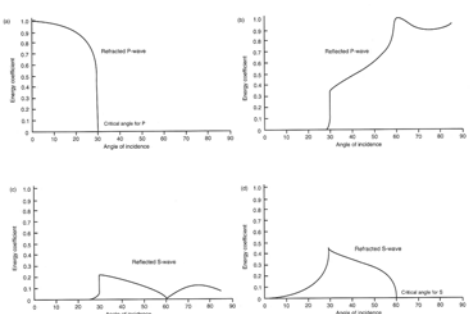

Figure 2-25 Partitioning of energy at an interface from an incident P-wave. As critical angles exist for both P- and S-waves, the velocity V_1 must be less than V_2. For this particular case $V_2/V_1 = 1.5$ and $\rho_2/\rho_1 = 0.5$.

Seismic Sources: Energy and Frequency

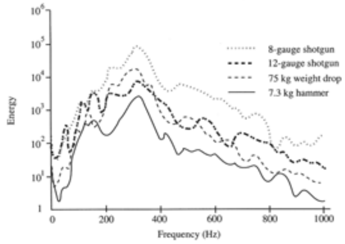

Figure 2-26 A comparison of relative energies and frequency content for shotgun and weight-drop seismic sources.

Seismic Sources: Energy

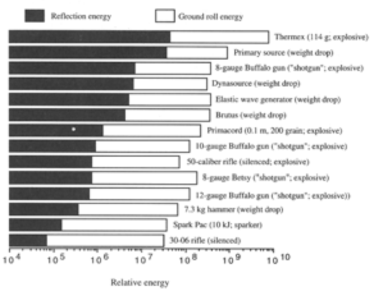

Figure 2-27 A plot of relative energies from various sources determined under uniform conditions at an experimental site. Based on information in Miller et al. (1986, p. 2067–2092).

Geophones

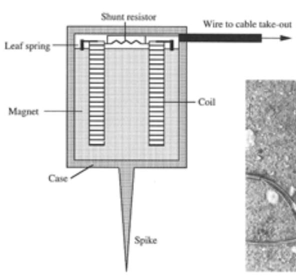

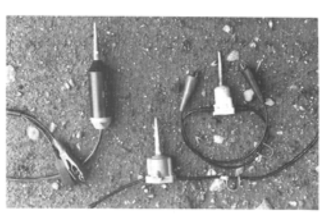

Figure 2-29 Photograph of typical geophones used for shallow exploration work. From left to right: 14-Hz phone, 30-Hz phone, and 50-Hz phone with marsh case. Each geophone has a spike for insertion into ground and two clips for connecting to seismic cable.

Geophone: Response Curve

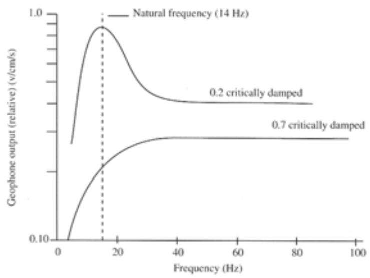

Figure 2-30 Response curves for 14-Hz geophone. 0.2 critical damping still produces a much greater response at the geophone's natural frequency than at other frequencies. 0.7 critical damping produces a more or less equal response to all frequencies above the natural frequency.

Geophone: Response Curve

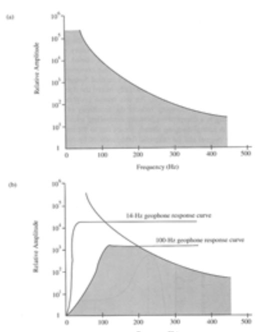

Seismograph Schematic

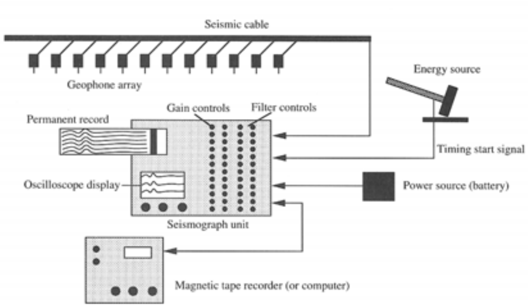

Figure 2-32 Diagrammatic representation of basic components of seismic exploration equipment.

Frequency Spectrum: Filtered

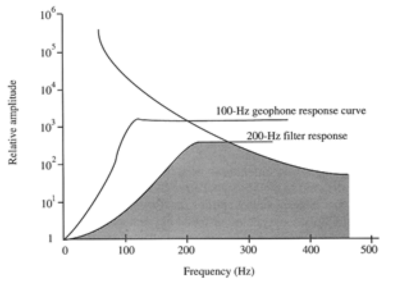

Figure 2-33 Frequency spectrum sampled by combination of 100-Hz geophone and 200-Hz filter.

Frequency Spectrum: Filtered

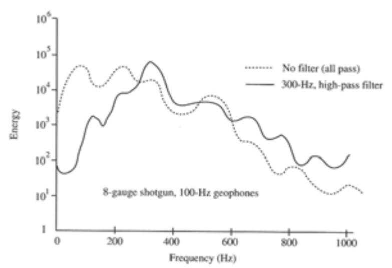

Figure 2-34 Effect of filtering on relative energies for frequency spectrum produced by 8-gauge shotgun source. Based on data in Pullan and MacAulay (1987).

Digital Sampling